Sulfonylureas blockade of neural and cardiac HERG channels

Barbara Rosati, Marcella Rocchetti, Antonio Zaza, Enzo Wanke*

Dipartimento di Fisiologia e Biochimica Generali, Università degli Studi di Milano, Via Celoria 26, 20133 Milan, Italy

Received 7 September 1998; received in revised form 26 October 1998

Abstract The human *ether-a-go-go*-related gene (*herg*) encodes a K^+ current (I_{HERG}) which plays a fundamental role in heart excitability and in neurons by contributing to action potential repolarization and to spike-frequency adaptation, respectively. In this paper we show that I_{HERG}, recorded in neuroblastoma cells and guinea-pig ventricular myocytes, was reversibly inhibited by the K_{ATP} channel blocker glibenclamide ($IC_{50} = 74$ μM). The voltage and use dependence of glibenclamide blockade were also evaluated. Another sulfonylurea, glimepiride, had less effective results in blocking I_{HERG}. The findings of this study are relevant to the interpretation of glibenclamide effects on cellular electrophysiology and suggest that oral antidiabetic therapy with sulfonylureas may contribute to iatrogenic QT prolongation and related arrhythmias.

Key words: Glibenclamide; K^+ channel; HERG channel; Cardiac cell

1. Introduction

Sulfonylurea compounds, such as glibenclamide, are blockers of the K^+ current sensitive to intracellular ATP ($I_{K(ATP)}$) widely used in the treatment of non-insulin-dependent diabetes mellitus. Long-QT syndrome, secondary to antidiabetic therapy with glibenclamide, has been recently reported [1]. This implies an action of glibenclamide on repolarizing currents.

Based on the assumption of a selective effect of glibenclamide on cardiac I_{KATP} (IC_{50} of 5–10 μM), this drug has been extensively used as a pharmacological tool in investigating the pathophysiology of ischemia [2]. However, glibenclamide also blocks the cardiac cAMP-activated chloride conductance, the cystic fibrosis conductance regulator chloride (CFTR) currents ($IC_{50} = 30$ μM) [3–5] and a Ca^{2+}- and ATP-independent K^+ current in a human neuroblastoma cell line [6]. Interference of glibenclamide with delayed rectifier currents, undetected so far, would be particularly relevant to the use of glibenclamide as a research tool.

The present work investigates the effects of glibenclamide on neuronal and cardiac K^+ currents, with a focus on the channel (I_{HERG} or I_{Kr}) encoded by the human *ether-a-go-go*-related gene (*herg*) [7–9]. The functional role of I_{HERG} (I_{Kr}) in the control of repolarization in the heart and in spike-frequency accommodation in the nervous system [10,11] motivates the interest in its modulation by glibenclamide. Neuroblastoma cells intrinsically expressing I_{HERG} [12–14] were ideally suited to test the dose dependence, mode of blockade and effects on resting potential (V_{REST}). Experiments on cardiac myocytes allowed a comparison of glibenclamide effect on the rapid (I_{Kr}) and slow components (I_{Ks}, encoded by *minK* and *KvLQT1* genes) [15,16] of the delayed rectifier current. The impact of glibenclamide-induced channel blockade on repolarization was also tested in this cell type.

2. Materials and methods

2.1. Cell culture and isolation

Experiments were carried out on cultured neuroblastoma cells and on freshly dissociated guinea-pig ventricular myocytes. The rat dorsal root ganglia (DRG) × murine neuroblastoma hybrid cell line F11, and the human neuroblastoma SH-SY5Y were cultured in Dulbecco's modified Eagle's medium (DMEM), containing 4.5 g/l of glucose and 10% fetal calf serum (FCS). Cells were incubated at 37°C in a humidified atmosphere with 5% CO_2 (10% for SH-SY5Y). Guinea-pig ventricular myocytes were freshly dissociated according to a previously described procedure [17] and preserved in a low Ca^{2+} medium at 4°C until use.

2.2. Patch clamp recordings

Membrane currents and voltage were recorded (Axopatch 200A, Axon, Foster City, CA, USA) in the whole-cell configuration by using pipettes with tip resistance in the range of 2–4 MΩ. Series resistance and capacitance were compensated to about 80–90% of their initial value. The pipette junction potential was not corrected. Cells were perfused through a microperfusion system allowing for solution changes to occur within 1 s approximately. While neuronal currents were studied at room temperature, reliable measurements of cardiac ones required temperatures in the physiological range (36 ± 0.5°C).

2.3. Protocols

In neuroblastoma cells I_{HERG} were elicited at $[K^+]_o = 40$ mM from a holding potential (V_H) of 0 mV as tail currents tested at −120 mV, as previously reported [11–14]. In cardiac cells delayed rectifier K^+ currents were activated by step depolarizations from V_H of −40 mV. The amplitude of I_{Kr} during the depolarizing step reflects the interplay between channel activation and inactivation; thus, drug effects were generally tested on tail currents recorded upon returning to negative potentials, which should be affected by channel activation only [18]. Potential interference by other currents was minimized by examining outward tail currents in ventricular myocytes (test potential −40 mV, $[K^+]_o = 4$ mM). In the cardiac cells contamination by Ca^{2+} currents was prevented by adding nisoldipine (0.2 μM) to all solutions. The rapid (I_{Kr}) and slow (I_{Ks}) components of the delayed rectifier current were dissected by means of both voltage protocols and the use of channel blockers E-4031 (specific for I_{Kr}) and chromanol 293B (specific for I_{Ks}) [19]. In some cases, glibenclamide effects were expressed by comparing glibenclamide-sensitive current ($I_{glib} = I$ in control minus I in glibenclamide) to currents sensitive to E-4031 (I_{E-4031}) and chromanol (I_{293B}), that can be safely assumed to reflect I_{Kr} and I_{Ks}, respectively. In both neural and cardiac cells, activation curves were constructed by measuring the amplitude of tail currents following long (steady-state) pulses at various potentials. Average normalized tail amplitudes were best fitted with Boltzmann functions and the relevant parameters were estimated.

2.4. Solutions

For neuronal cells the standard extracellular solution contained (mM): NaCl 130, KCl 5, $CaCl_2$ 2, $MgCl_2$ 2, HEPES-NaOH 10, D-glucose 5, pH 7.4. When necessary, the NaCl was replaced by KCl to $[K^+]_o = 40$ mM. The standard pipette solution at $[Ca^{2+}]_i = 10^{-7}$ M (p*Ca* 7) contained (mM): K^+-aspartate 130, NaCl 10, $MgCl_2$ 2, $CaCl_2$ 1.3, EGTA-KOH 10, HEPES-KOH 10, ATP (Mg^{2+} salt) 1, pH 7.3.

*Corresponding author. Fax: (39) (2) 70632884.
E-mail: enzo.wanke@unimi.it

PII: S0014-5793(98)01444-6

For cardiac cells the standard extracellular solution contained (mM): NaCl 154, KCl 4, $CaCl_2$ 2, $MgCl_2$ 1, HEPES-NaOH 5, D-glucose 5.5, pH 7.35. The pipette solution contained (mM) K^+-aspartate 110, KCl 23, EGTA-KOH 1, $CaCl_2$ 0.4 (p*Ca* 7), $MgCl_2$ 3, HEPES-KOH 5, GTP (Na^+ salt) 0.4, ATP (Na^+ salt) 5, creatine phosphate 5, pH 7.3. In evaluating I_{Kr}, I_{Ks} contamination was minimized by adding the specific blocker chromanol 293B (10 μM) [19] to all solutions. In evaluating I_{Ks}, I_{Kr} contamination was removed by adding 5 μM E-4031, the specific blocker of I_{Kr}.

Glibenclamide (RBI), glimepiride (a kind gift from Dr. P. Marchetti) and chromanol 293B were dissolved in DMSO, nisoldipine in ethanol and E-4031 and WAY 123,398 (Wyeth-Ayerst Research, Princeton, NJ, USA) in water. Stock solutions of each substance were diluted in extracellular solution to the desired concentration. Ethanol and DMSO, present at final concentrations ≤0.1%, were included in control as well as test solutions. Nisoldipine, E-4031 and chromanol 293B were generous gifts from Bayer Pharmaceuticals, Sanofi Recherche and Roche Pharmaceuticals, respectively.

2.5. Statistical analysis

The Student's *t*-test was used to compare differences between sample means. Best fits of experimental points to Hill and Boltzmann functions were obtained by non-linear, least-square fitting routines (Microcal Origin). Differences between fitted curves were tested by considering the overlap between their 0.05 confidence intervals. Significance was defined by $P < 0.05$. Results are presented as mean ± S.E.M.

3. Results

3.1. Experiments in neuroblastoma cells

3.1.1. Glibenclamide blockade of I_{HERG} and its dose-dependence. The effect of 1 min glibenclamide superfusion on I_{HERG} in F11 cells is shown in Fig. 1A. Changes were fully reversible within 2 min of washout and were reproduced by a second application of the drug. Similar results were obtained in the human neuroblastoma SH-SY5Y (not shown).

The effect of glibenclamide (100 μM) on V_{REST} [13,14] which in neuroblastoma cells is governed by I_{HERG} [12], was tested under current-clamp conditions ($I = 0$). A representative record from such an experiment is shown in Fig. 1B. The average depolarization induced by glibenclamide (8 ± 2.2 mV, $n = 5$; $P < 0.05$) was comparable to that caused in the same cell type by other HERG channel blockers [13].

The dose-response relationship of glibenclamide effect on I_{HERG} in F11 cells is shown in Fig. 1C. Data obtained in SH-SY5Y did not differ significantly (not shown). Fractional current inhibition at each concentration was expressed as unity minus the ratio between current amplitudes measured under test and control conditions. Fractional inhibition values were best fitted by the Hill function $(1+([IC_{50}]/[glib])^p)^{-1}$, where [glib] is glibenclamide concentration, IC_{50} is [glib] exerting 50% inhibition, and '*p*' is the Hill number. The fitting procedure estimated a glibenclamide IC_{50} of 74.8 ± 7 μM with $p = 0.82 \pm 0.05$. Glimepiride, another sulfonylurea drug, was also tested for comparison. The results are reported in Fig. 1C for concentrations of 10, 50, 100 and 500 μM. Glimepiride appeared to be about ten times less effective than glibenclamide in blocking I_{HERG}. We were not able to test higher glimepiride concentrations because it became insoluble and precipitated in the perfusion tubes.

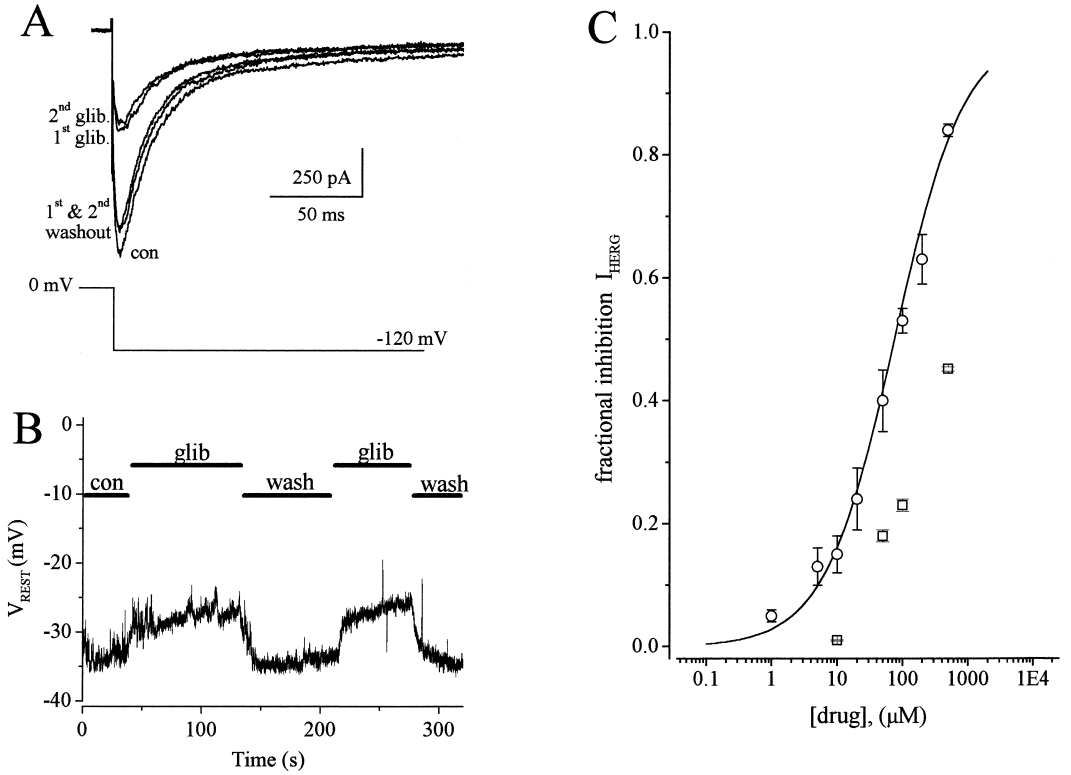

Fig. 1. Glibenclamide blockade of I_{HERG} in neuronal cells. A: Reversibility of block. I_{HERG} was elicited by stepping to −120 mV from a holding potential of 0 mV (see below); glibenclamide (100 μM) was applied twice (1st and 2nd glib) for 60-s periods followed by 2 min washout (1st and 2nd washout). B: Time course of changes in resting membrane potential (V_{REST}) of an F11 cell during 90 s superfusion with glibenclamide (marked by the bars). C: Fractional inhibition of I_{HERG} tail currents by glibenclamide concentrations of (μM): 1 ($n = 5$), 5 ($n = 4$), 10 ($n = 5$), 20 ($n = 7$), 50 ($n = 11$), 100 ($n = 6$), 200 ($n = 2$), 500 ($n = 2$). The solid line represents best fit of data points with Hill function (see text for parameters). Data obtained with glimepiride concentrations of (μM) 10 ($n = 3$), 50 ($n = 5$), 100 ($n = 5$), 500 ($n = 3$) are reported (□) in the same diagram for comparison.

3.1.2. Voltage and use dependence of I_{HERG} blockade. In order to investigate the mode of glibenclamide action we tested if (i) the voltage dependence of I_{HERG} activation and inactivation were modified by the drug; and (ii) if, similarly to other organic I_{HERG} blockers [20], glibenclamide effect was use-dependent.

Fig. 2A shows average activation curves obtained from 4 cells under control conditions and during superfusion with glibenclamide; activation parameters were estimated from Boltzmann fits of average experimental points. The membrane potential required for 50% current activation ($V_{0.5}$) and the Boltzmann slope (k) were −35 mV and 6.6 mV, respectively, in control and −38.7 and 7.8 mV, respectively, during exposure to glibenclamide. However, these differences appeared not to be significant. The properties of the other voltage-dependent gate, namely inactivation [13], were tested in 3 cells. Inactivation parameters $V_{0.5}$ and k were, respectively, −38.6 and 21.9 mV in control and −39.6 and 27.2 mV during glibenclamide delivery. These differences were again not significant.

Use dependence of the glibenclamide effect on I_{HERG} was studied with the protocol shown in Fig. 2B. Superimposition of tail currents from individual pulses (Fig. 2C) shows that the glibenclamide effect, present at the first pulse, was unchanged in the following ones. This is at variance with the progressive development of blockade during subsequent pulses of the train, induced by the use-dependent I_{HERG} blocker WAY 123,398 (Fig. 2C, inset) [21]. The reduction of the outward current at +10 mV, which can be observed during glibenclamide application, is due to blockade of a delayed rectifier K^+ current by the drug [6]. This effect cannot be seen in Fig. 1A, since the delayed rectifier current is inactivated ($V_H = 0$ mV).

3.2. Experiments on cardiac ventricular myocytes

Since ventricular myocytes express two types of delayed rectifier current (I_{Kr} and I_{Ks}), in these cells glibenclamide effects were best described by comparison with those of selective blockers of each component (E-4031 and chromanol 293B).

3.2.1. Comparison of the effects of glibenclamide and E-4031 on I_{Kr} (HERG). In evaluating I_{Kr}, relatively short depolarizing steps were delivered every 4 s within a range of potentials at which I_{Ks} activation was negligible [22]; the effect of 100 μM glibenclamide was compared with that of a saturating

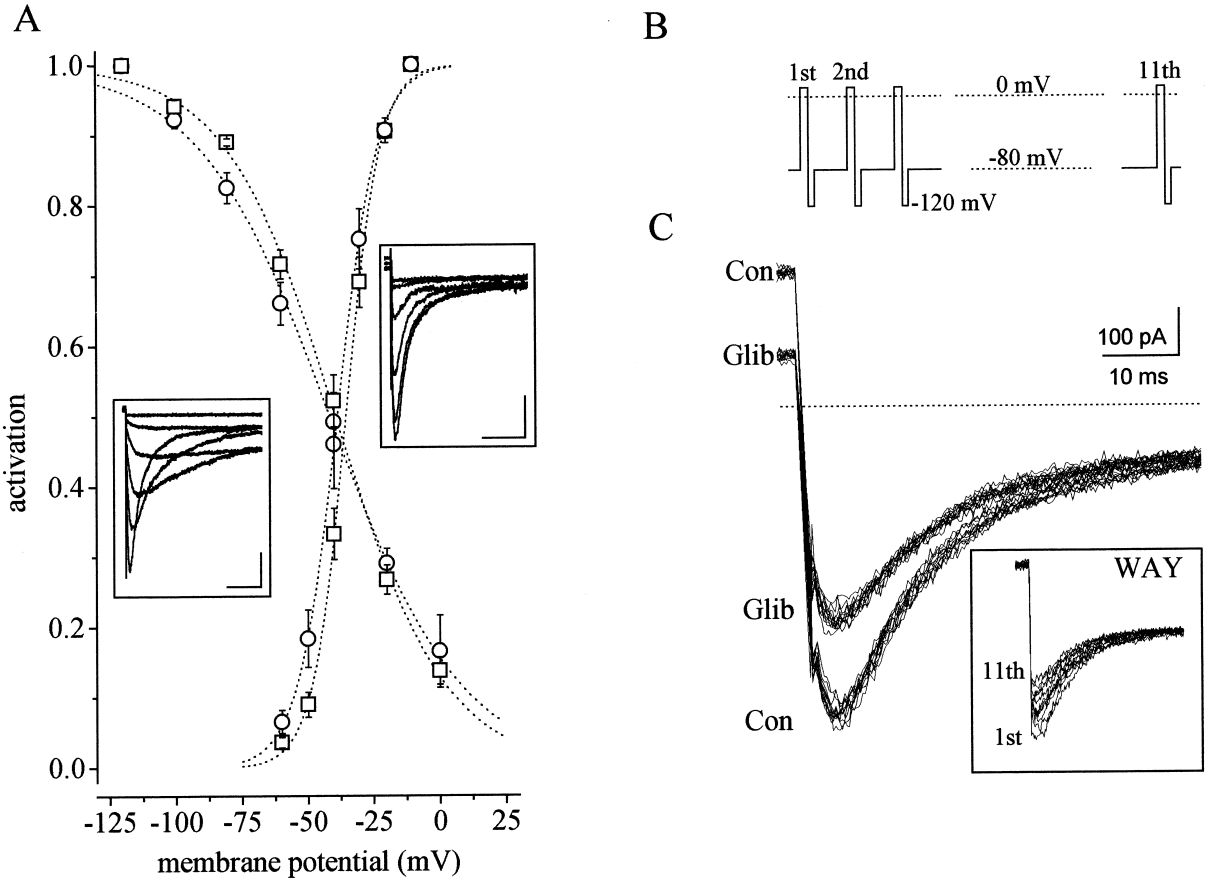

Fig. 2. Voltage and use dependence of glibenclamide blockade of I_{HERG} in F11 neuroblastoma cells. A: Steady-state I_{HERG} activation curve in control (□) and during 100 μM glibenclamide (○). For activation, tail current amplitudes were measured at −120 mV after long conditioning steps in the range −10 to −60 mV (see inset). Dotted lines are Boltzmann fits of average experimental points ($n = 4$). For inactivation, from a holding potential of 0 mV steps were applied in the range +20 to −120 mV. Tail current amplitudes (shown in the left inset) were divided for the driving force to determine HERG conductance. The mean values obtained ($n = 3$) are fitted with Boltzmann curves (dotted lines). Scalers in left and right insets represent 50 ms and 300 pA. B: Protocol used to investigate the use dependence of I_{HERG} blockade; an activating step (+10 mV, 330 ms) was followed by a test pulse (−120 mV, 270 ms); this protocol was applied in runs of 11 episodes at a cycle length of 2 s; C: Superimposed I_{HERG} tails recorded during individual episodes (from 1 to 11) in control (con) and during 100 μM glibenclamide (glib). The difference in the outward current at +10 mV is due to partial block of a K^+ delayed rectifier current by glibenclamide (see text). The inset shows the same use-dependence protocol applied during steady-state superfusion with 1 μM WAY 123,398.

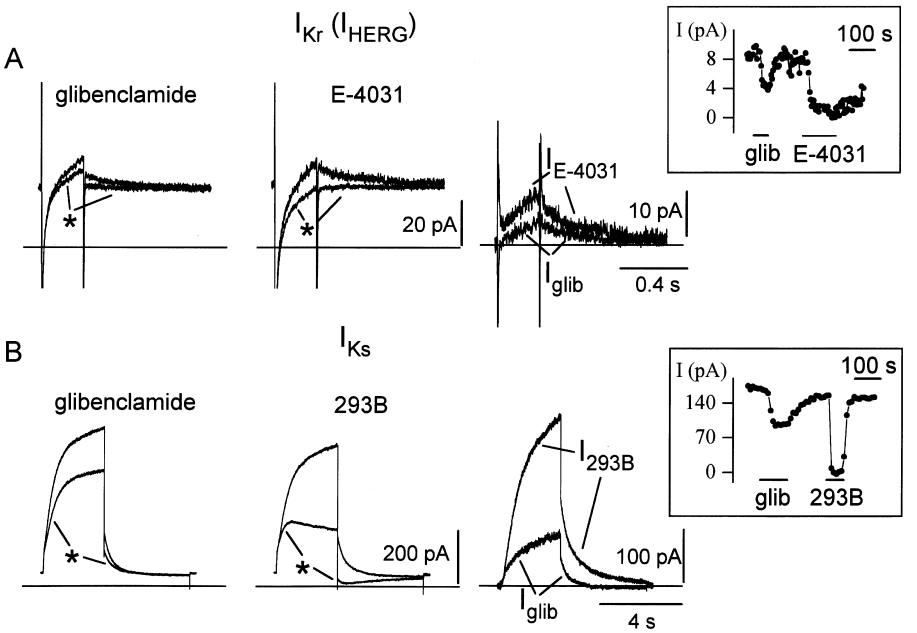

Fig. 3. Effects of 100 μM glibenclamide on I_{Kr} and I_{Ks} in cardiac ventricular myocytes. Current traces in control and during drug superfusion (*) are compared in each of the first two panels; in the third panel control and test traces are subtracted to yield drug-sensitive currents (I_{E4031}, I_{glib} and I_{293B}). The insets show plots of tail current amplitude vs. time measured throughout the experiment; the time of drug superfusion is marked by bars (glib 100 μM, E4031 5 μM; chromanol 293B 10 μM). A: I_{Kr} (HERG) was activated by 250-ms steps to 0 mV from a holding potential of −40 mV (interval 4 s) in the presence of nisoldipine and chromanol 293B. B: I_{Ks} was activated by 3-s steps to +30 mV from a holding potential of −40 mV (interval 10 s) in the presence of nisoldipine and E-4031.

concentration (5 μM) of the specific I_{Kr} blocker E-4031 [22]. A representative result of this experiment is shown in the upper panels of Fig. 3. Glibenclamide, 100 μM, reduced I_{Kr} tail amplitude from 13.75 ± 2.44 pA to 5.28 ± 0.981 pA (−61.6 ± 1.4%; $n = 5$; $P < 0.05$). After washout, the current returned to 12.06 ± 1.36 pA (N.S. vs. control) (Fig. 3A). The amplitude of I_{Kr} tail currents was reduced by E-4031 from 16.89 ± 2.93 pA to 1.64 ± 0.91 pA (−86.8 ± 6.5%; $n = 6$; $P < 0.05$). As previously described [23], reversal of the E-4031 effect upon washout was slow and incomplete and could be observed in 3 out of 6 cells (10.97 ± 3.6 pA) (not shown).

A comparison between the voltage dependence of I_{Kr} and of the current sensitive to glibenclamide was performed by obtaining activation curves for I_{glib} ($n = 4$) and I_{E-4031} ($n = 5$). As tested by taking into account the 0.05 confidence limits of the fitting functions, the normalized activation curves of I_{glib} and I_{E-4031} did not differ significantly. For I_{glib} and I_{E-4031} $V_{0.5}$ values were 13.6 and 12.1 mV, respectively; Boltzmann slopes were 10.4 and 8.3 mV. The maximum current densities, as estimated from fits of raw data, were 0.409 pA/pF for I_{E-4031} and 0.339 pA/pF for I_{glib} (not shown).

3.2.2. Comparison of the effects of glibenclamide and chromanol 293B on I_{Ks}. With the purpose of evaluating the specificity of glibenclamide effects for either component of the delayed rectifier current, we also tested drug effects on I_{Ks}. Such effects were compared to those of the specific I_{Ks} blocker chromanol 293B (10 μM) [19]. The results of this experiment are exemplified in the bottom panels of Fig. 3. Relatively long (3-s) depolarizing steps were used to activate I_{Ks}. The effect of glibenclamide was expressed relative to those of chromanol 293B, i.e. by comparing I_{glib} to chromanol-sensitive current (I_{293B}). Densities of I_{293B} and I_{glib} tail currents were 1.27 ± 0.36 pA/pF and 0.41 ± 0.14 pA/pF ($n = 5$; $P < 0.05$), respectively. Thus, on average, I_{glib} was 30.85 ± 2.72% of I_{293B}. The effects of both glibenclamide and chromanol 293B were largely reversible upon washout (Fig. 3B, inset).

3.2.3. Effect of glibenclamide on ventricular action potential duration. In order to investigate the functional significance of glibenclamide effects on delayed rectifier currents, we tested the effect of this drug on action potentials recorded under I-clamp conditions ($I = 0$) during stimulation at a cycle length of 1 s. Action potential duration (APD) was measured at 90% of repolarization. An example of glibenclamide effect on APD is shown in panel A of Fig. 4. Superfusion with glibenclamide, 100 μM, reversibly prolonged APD by 9.4 ± 1% (163.9 ± 10.2 ms vs. 150.5 ± 9.9 ms; $n = 14$; $P < 0.05$). Even if glibenclamide blockade of I_{Ks} was small, as compared to that of I_{Kr}, both effects might contribute to APD prolongation, depending on the proportion of delayed rectifier current accounted for by each component. To address this issue, we tested the extent of APD prolongation resulting from the specific inhibition of I_{Ks} by 10 μM chromanol 293B (Fig. 4B) and of I_{Kr} by 5 μM E-4031 (Fig. 4C). APD was prolonged by E-4031 from 148.3 ± 9.9 ms to 184.6 ± 11.6 ms (24.8 ± 3.3%; $n = 14$; $P < 0.05$) and by chromanol 293B from 152.5 ± 12.1 ms to 160.35 ± 12.5 ms (5.3 ± 1.6%; $n = 9$; $P < 0.05$). Thus, under the present experimental conditions, the effect of glibenclamide on APD may largely result from I_{Kr} (I_{HERG}) inhibition.

4. Discussion

The present work shows that glibenclamide blocks neural and cardiac delayed rectifier K^+ currents and prolongs cardiac repolarization. Although the drug also partly inhibited the slow component of the cardiac delayed rectifier current (I_{Ks}), its effects on the HERG type channel (I_{Kr}, I_{HERG}) were more prominent and likely to account for most of the APD prolongation.

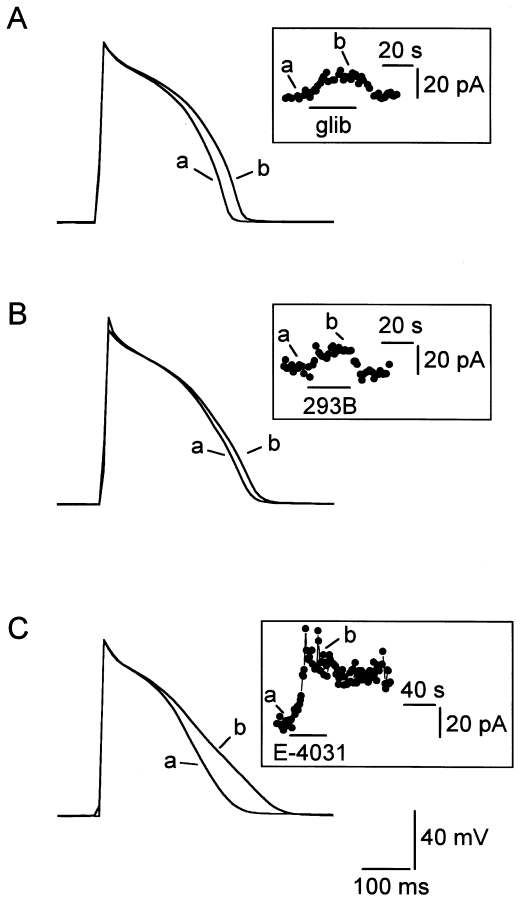

Fig. 4. Effect of glibenclamide (glib), I_{Ks} and I_{Kr} blockers on cardiac action potentials. Action potentials recorded in control and during steady-state drug superfusion are superimposed. The insets show the time course of APD_{90} values measured throughout the experiment (time of drug superfusion marked by bars). A: Glibenclamide, 100 μM; B: chromanol 293B, 10 μM; C: E4031, 5 μM.

4.1. Dose dependence

Glibenclamide inhibited I_{HERG} in neuroblastoma cells with a threshold concentration of 10 μM and an IC_{50} of 75 μM (Fig. 1). The Hill coefficient suggests a 1:1 stoichiometry for the drug-channel interaction. Glimepiride seemed to be less effective in blocking I_{HERG}, requiring a threshold concentration of 50 μM. The extent of inhibition of cardiac I_{Kr} by 100 μM glibenclamide (61%) was consistent with the dose dependence measured in neuroblastoma cells (60% at 100 μM). Glibenclamide concentrations inhibiting I_{HERG}, I_{Kr} and I_{Ks} were higher than those active on I_{KATP} in pancreatic β-cells (in the nM range) [24], but closer to those required to inhibit cardiac I_{KATP} (1–100 μM) [25–27].

4.2. Mode of I_{HERG} (I_{Kr}) blockade

Failure to affect the voltage dependence of activation and the lack of use dependence of blockade shows that glibenclamide action on I_{HERG} (I_{Kr}) was not influenced by the gating state. This, and the fast development of effects, suggest that glibenclamide may bind to a channel domain exposed to the extracellular environment. This is at variance with what was reported for the slowly developing action of glibenclamide on cAMP-activated Cl-currents [4]. The mode and dose dependence of glibenclamide action were remarkably similar between neural and cardiac HERG-type currents, thus suggesting common pharmacological properties between the channel expressed in the two tissues.

Although to a lesser extent, I_{Ks} was also inhibited by glibenclamide. It has been recently proposed that a subunit of the I_{Ks} channel (minK) may also contribute to functional expression of I_{Kr} [28]. On the other hand, drug effects on delayed rectifier current and I_{KATP} appear to be closely coupled in smooth muscle [29]. Thus, the low selectivity of the glibenclamide effect might reflect the presence of specific 'receptors' for this drug on all such channels. Indeed, the existence of sulfonylurea receptors (SUR1, SUR2) with very different affinities for glibenclamide [30] which are crucial in the formation (with the K^+ channel Kir 6.2) of the pancreatic, neural and muscle ATP-sensitive K^+ channels is well documented . This finding could suggest that the HERG channels could also be linked to these receptors. Moreover, our data, showing that both I_{Kr} and I_{Ks} (to a much lesser extent) are affected by glibenclamide, could be explained also in another way: both these channels have been shown to complex with minK proteins [28] and putatively either minK and/or SUR could form heteromultimer functional complexes. However, while this remains a matter of speculation, it is difficult to rule out that the widespread channel blocking effects of glibenclamide may result from some non-specific property of the molecule.

4.3. Relevance and implications

Glibenclamide concentrations in the 10–100-μM range are often used to test the role of I_{KATP} in cardiac cellular electrophysiology both under normal [25] and ischemic conditions [27] (for review see [31] and [32]). Blockade of cardiac delayed rectifier currents, described in the present study, might mimick the effects expected from I_{KATP} blockade, thus potentially confusing the interpretation of results.

The hypoglycemic action of glibenclamide, i.e. blockade of I_{KATP} in pancreatic β-cells, is reported to occur at concentrations in the nanomolar range [24]. Thus, although iatrogenic long-QT syndrome during glibenclamide therapy has been reported [1], it seems unlikely that glibenclamide alone may be a widespread cause of clinical proarrhythmia. Nonetheless, it is difficult to rule out that preexisting primary or iatrogenic long-QT syndromes may be unmasked or accentuated by the drug. A similar phenomenon has been described for various agents (e.g. antiarrhythmic drugs, antihistamines, macrolids, antiserotoninergics, antipsychotics, etc.) [33–35] whose effects on cardiac delayed rectifier currents caused serious arrhythmias when drugs were administered either in association or to abnormally sensitive individuals. In this respect, the use of glimepiride, which was also reported to have less cardiovascular side effects in vivo [36], should be taken into account.

References

[1] Ikeda, T. (1994) Diabetes Metab. 20, 565–567.
[2] Gross, G.J. and Auchampach, J.A. (1992) Cardiovasc. Res. 26, 1011–1016.
[3] Ripoll, C., Lederer, W.J. and Nichols, C.G. (1993) J. Cardiovasc. Electrophysiol. 4, 38–47.
[4] Tominaga, M., Horie, M., Sasayama, S. and Okada, Y. (1995) Circ. Res. 77, 417–423.
[5] Sheppard, D.N. and Welsh, M.J. (1992) J. Gen. Physiol. 100, 573–591.
[6] Reeve, H.L., Vaughan, P.F. and Peers, C. (1992) Neurosci. Lett. 135, 37–40.

[7] Titus, S.A., Warmke, J.W. and Ganetzky, B. (1997) J. Neurosci. 17, 875–881.
[8] Trudeau, M.C., Warmke, J.W., Ganetzky, B. and Robertson, G.A. (1995) Science 269, 92–95.
[9] Warmke, J.W. and Ganetzky, B. (1994) Proc. Natl. Acad. Sci. USA 91, 3438–3442.
[10] Sanguinetti, M.C., Jiang, C., Curran, M.E. and Keating, M.T. (1995) Cell 81, 299–307.
[11] Chiesa, N., Rosati, B., Arcangeli, A., Olivotto, M. and Wanke, E. (1997) J. Physiol. 501, 313–318.
[12] Arcangeli, A., Bianchi, L., Becchetti, A., Faravelli, L., Coronnello, M., Mini, E., Olivotto, M. and Wanke, E. (1995) J. Physiol. 489, 455–471.
[13] Faravelli, L., Arcangeli, A., Olivotto, M. and Wanke, E. (1996) J. Physiol. 496, 13–23.
[14] Bianchi, L., Wible, B., Arcangeli, A., Taglialatela, M., Morra, F., Castaldo, P., Crociani, O., Rosati, B., Faravelli, L., Olivotto, M. and Wanke, E. (1998) Cancer Res. 58, 815–822.
[15] Barhanin, J., Lesage, F., Guillemare, E., Fink, M., Lazdunski, M. and Romey, G. (1996) Nature 384, 78–80.
[16] Sanguinetti, M.C., Curran, M.E., Zou, A., Shen, J., Spector, P.S., Atkinson, D.L. and Keating, M.T. (1996) Nature 384, 80–83.
[17] Zaza, A., Rocchetti, M., Brioschi, A., Cantadori, A. and Ferroni, A. (1998) Circ. Res. 82, 947–956.
[18] Smith, P.L., Baukrowitz, T. and Yellen, G. (1996) Nature 379, 833–836.
[19] Busch, A.E., Suessbrich, H., Waldegger, S., Sailer, E., Greger, R., Lang, H., Lang, F., Gibson, K.J. and Maylie, J.G. (1996) Pflügers Arch. 432, 1094–1096.
[20] Spector, P.S., Curran, M.E., Keating, M.T. and Sanguinetti, M.C. (1996) Circ. Res. 78, 499–503.
[21] Spinelli, W., Moubarak, I.F. and Parson, R.W. (1993) Cardiovasc. Res. 27, 1580–1591.
[22] Sanguinetti, M.C. and Jurkiewicz, N.K. (1990) J. Gen. Physiol. 96, 195–215.
[23] Verheijck, E.E., van Ginneken, A.C.G., Bourier, J. and Bouman, L.N. (1995) Circ. Res. 76, 607–615.
[24] de Weille, J.R. (1992) Cardiovasc. Res. 26, 1017–1020.
[25] Faivre, J.F. and Findlay, I. (1989) Biochim. Biophys. Acta 984, 1–5.
[26] Kantor, P.F., Coetzee, W.A., Carmeliet, E.E., Dennis, S.C. and Opie, L.H. (1990) Circ. Res. 66, 478–485.
[27] Venkatesh, N., Lamp, S.T. and Weiss, J.N. (1991) Circ. Res. 69, 623–637.
[28] McDonald, T.V., Yu, Z., Ming, Z., Palma, E., Meyers, M.B., Wang, K.W., Goldstein, S.A. and Fishman, G.I. (1997) Nature 388, 289–292.
[29] Edwards, G., Ibbotson, T. and Weston, A.H. (1993) Br. J. Pharmacol. 110, 1037–1048.
[30] Aguilar-Bryan, L., Clement, J.P., Gonzalez, Kunjilwar, K., Babenko, A. and Bryan, J. (1998) Physiol. Rev. 78, 227–245.
[31] Wilde, A.A. and Janse, M.J. (1994) Cardiovasc. Res. 28, 16–24.
[32] Schotborgh, C.E. and Wilde, A.A. (1997) Cardiovasc. Res. 34, 73–80.
[33] Zehender, M., Hohnloser, S. and Just, H. (1991) Cardiovasc. Drugs Ther. 5, 515–530.
[34] Iwahashi, K. (1996) Clin. Neuropharmacol. 19, 267–270.
[35] Rosen, M.R. (1996) Circulation 94, 607–609.
[36] Geisen, K., Vegh, A., Krause, E. and Popp, J.G. (1996) Horm. Metab. Res. 28, 496–507.